Clarification of the Mechanism of Interfacial Electron-Transfer Reaction between Ferrocene and Hexacyanoferrate(III) by Digital Simulation of Cyclic Voltammograms

Hiroki Hotta, Seiko Ichikawa, Takayasu Sugihara, and Toshiyuki Osakai*

Department of Chemistry, Faculty of Science, Kobe University, Nada, Kobe 657-8501, Japan

Received: April 21, 2003; In Final Form: May 1, 2003

The reaction mechanism of electron transfer (ET) between ferrocene (Fc) in nitrobenzene (NB) and $Fe(CN)_6^{3-}$ in water (W) was clarified by digital simulation of cyclic voltammograms. The voltammograms observed under various concentration conditions could not be elucidated by assuming a heterogeneous ET at the NB/W interface, whereas they were successfully elucidated in terms of the ion-transfer (IT) mechanism, in which a homogeneous ET between $Fe(CN)_6^{3-}$ and Fc (partially distributed from NB) occurs in the W phase and the interfacial transfer of the resultant ferricenium ion (Fc^+) is responsible for the current passage across the interface. The validity of the IT mechanism was further supported by spectroscopic detection of Fc^+ produced in the W phase without electrochemical control. These results show that the homogeneous ET proceeds more advantageously than the heterogeneous ET due to a pinpoint collision of redox species at the interface. This may be ascribed to the difference in the volume of reaction field between the homogeneous and heterogeneous ETs. The reaction field for the former has a thickness of ca. 200 μm, whereas that for the latter is restricted to an interfacial layer as thin as several ångstroms. Such a large difference in the volume of the reaction field would overcome the disadvantage of the IT mechanism, i.e., the small partition of Fc into the W phase. The low possibility of the ET mechanism has also been deduced from theoretical estimation of the standard rate constant and transfer coefficient for the hypothetical heterogeneous ET.

Introduction

Clarification of the mechanism of electron transfer (ET) at the oil (O)/water (W) (or liquid/liquid) interface is fundamentally important for understanding energy conversion in biomembranes (e.g., respiratory chain, photosynthesis, etc.).[1,2] Samec et al.[3] first employed cyclic voltammetry to observe an interfacial redox reaction between ferrocene (Fc) in nitrobenzene (NB) and $Fe(CN)_6^{3-}$ in W:

$$Fc(O) + Fe(CN)_6^{3-}(W) \rightleftharpoons Fc^+(O) + Fe(CN)_6^{4-}(W) \quad (1)$$

Since then, various interfacial ET reactions have been reported, involving other hydrophobic redox species, e.g., tetracyanoquinonedimethane,[4] lutetium and tin biphthalocyanines,[5,6] iron and ruthenium tetraphenylporphyrins,[7] and substituted ferrocenes,[8] etc. Furthermore, Kihara's group has reported several interesting biomimetic ET systems involving ascorbic acid,[9] flavin mononucleotide,[10] and β-nicotinamide adenine dinucleotide.[11]

However, reaction mechanisms of interfacial ETs are not necessarily as simple as shown in eq 1. For example, a possible complicated mechanism for the Fc−$Fe(CN)_6^{3-}$ system has been discussed:[12]

$$Fc(O) \rightleftharpoons Fc(W) \quad (2a)$$

$$Fc(W) + Fe(CN)_6^{3-}(W) \rightleftharpoons Fc^+(W) + Fe(CN)_6^{4-}(W) \quad (2b)$$

$$Fc^+(W) \rightleftharpoons Fc^+(O) \quad (2c)$$

In this so-called ion transfer (IT) mechanism, the interfacial transfer of ferricenium ion (Fc^+) being generated by a homogeneous ET reaction in W is responsible for the current passage across the interface. However, if all equilibria are quite mobile, the IT mechanism is not distinguishable from that described as a single-step ET (eq 1). Accordingly, kinetic behavior is essential for clarification of the ET reaction mechanism.

So far, certain efforts have been devoted to study the Fc−$Fe(CN)_6^{3-}$ system using cyclic voltammetry,[8,13,14] convolution potential sweep voltammetry,[15] current scan polarography,[4] ac impedance method,[16] voltammetry with micro liquid/liquid interfaces,[17] scanning electrochemical microscopy (SECM),[18] and laser trapping of a single oil droplet,[19] etc. Noteworthy kinetic behaviors were observed, particularly when the concentration of Fc was lower,[3,4] but were discussed mainly in terms of a simple heterogeneous ET such as eq 1. On the other hand, a recent microelectrochemical study with expanding droplets suggested an IT of Fc^+ generated in the Fc (1,2-dichloroethane)−$IrCl_6^{2-}$ (W) system.[20] This seems to support the IT mechanism shown by eqs 2a−2c, but no definitive conclusion has been drawn for the reaction mechanism.

In 1988, Geblewicz and Schiffrin[5] claimed that the first evidence was given for a true heterogeneous ET across the O/W interface using a highly hydrophobic, lutetium biphthalocyanine complex in the O phase. In subsequent studies,[6,7] other hydrophobic organometallic compounds were also claimed to show true ETs in the absence of possible IT. These experimental results then stimulated theoretical discussions by several researchers,[21−29] and the applicability of the theory proposed by Marcus has been tested by means of ac impedance measurements[30] and SECM.[31,32]

Recently, we have devised a new electrochemical system for characterizing ET processes at the O/W interface; this is named "electron conductor separating oil−water (ECSOW) system".[33]

* Corresponding author. Phone and Fax: +81-78-803-5682. E-mail: osakai@kobe-u.ac.jp.

10.1021/jp035058p CCC: $25.00
Published on Web 08/02/2003

In this system, the O and W phases are separated by an electron conductor (EC; e.g., Pt), and an ET process via the EC phase can be observed voltammetrically in a manner similar to the O/W interface. It should be noted that in the ECSOW system, no IT occurs through the EC phase. Although the ECSOW system is thermodynamically equivalent to the corresponding O/W interface, they may be different from a kinetic viewpoint. In practice, cyclic voltammograms of the $Fc-Fe(CN)_6^{3-}$ system at the nitrobenzene (NB)/W interface showed features different from those obtained with the ECSOW system, especially when the concentrations of the redox species in both phases were lower. Although the voltammograms for the ECSOW system could be elucidated in terms of a simple, reversible ET catalyzed by the EC phase, those for the NB/W interface suggested the existence of a kinetically controlled process. In this study, we have employed a digital simulation technique to show that the kinetic voltammograms with the NB/W interface can be elucidated in terms of the IT mechanism. Although the presently used, four-electrode cyclic voltammetry might be conventional, its combination with the digital simulation technique allows us to obtain no less information about the reaction mechanism than the recently introduced modern techniques. We have also attempted a discussion as to why heterogeneous ET did not occur at the interface, based on a theoretical estimation of the diffusion-controlled rate constant at the O/W interface.[34]

Experimental Section

Materials. Analytical grade reagents of ferrocene (Aldrich), $K_3Fe(CN)_6$ (Wako Pure Chemical Industries, Ltd.), $K_4Fe(CN)_6$ (trihydrate; Wako), and $Na_4Fe(CN)_6$ (Wako) were used as received. An aqueous solution of $Na_3Fe(CN)_6$ was prepared by electrolysis of an aqueous solution of $Na_4Fe(CN)_6$ with a flow column electrolytic cell (Hokuto Denko Co., HX-203); the electrolysis potential was +0.40 V vs Ag/AgCl (saturated KCl). The synthesis of tetrapentylammonium tetraphenylborate (TPnATPB), the preparation of an aqueous solution of tetrapentylammonium chloride (TPnACl; Tokyo Kasei Industry Co., Ltd.), and the purification of analytical grade nitrobenzene (Wako) were described previously.[35] All other reagents were of analytical grade and used as received.

Electrochemical Measurements. Cyclic voltammetric measurements with stationary NB/W interfaces were performed using a microcomputer-controlled four-electrode potentiostat (Hokuto Denko, HA1010mM1A), which was equipped with a positive feedback circuit for ohmic drop compensation.[36] The electrolytic cell used can be expressed as

	(W)	(NB)	(W)	(W)	
Ag/AgCl	0.02 M TPnACl	0.1 M TPnATPB	0.1 M LiCl	0.1 M LiCl	Ag/AgCl
(CE1)	0.1 M $MgSO_4$	*x* mM Fc	*y* mM $Na_3Fe(CN)_6$	0.1 M LiCl	(CE2)
			(*y*/5) mM $Na_4Fe(CN)_6$		

	(W)	(NB)	(W)	
Ag/AgCl	0.02 M TPnACl	0.1 M TPnATPB	0.1 M LiCl	Pt
(RE1)	0.1 M $MgSO_4$	*x* mM Fc	*y* mM $Na_3Fe(CN)_6$	(RE2)
			(*y*/5) mM $Na_4Fe(CN)_6$	

Cell A

where || represents the test NB/W interface (geometric area, 0.074 cm^2), the potential difference of which was controlled using the two reference electrodes (RE1 and RE2) immersed in the respective phases by means of Luggin capillaries whose tips were located near the NB/W interface. The solution resistance (~3.5 kΩ) between the tips of the Luggin capillaries was usually compensated for by 95%.[36] The current flowing through the test interface was detected by means of the two counter electrodes (CE1 and CE2). For each voltammetric scan, the test interface was renewed by pouring an aqueous solution from a reservoir.

For measurements with the ECSOW system, an EC phase was inserted between the NB and W phases (i.e., at the NB/W interface indicated by || in Cell A). This system can be feasibly realized by immersing in the NB and W phases two Pt disk electrodes connected by an electric wire.[33] Prior to each measurement, the electrode surfaces (area, 0.020 cm^2) were freshly polished with a 0.25 μm diamond slurry and rinsed with distilled water or acetone in an ultrasonic field. Voltammetric measurements with the ECSOW system were performed in a manner similar to those with the above NB/W interface, except that potassium salts of the hexacyanoferrates were used instead of the sodium salts.

Determination of the standard ion-transfer potential of Fc^+ at the NB/W interface was made by using the following cell:

	(W)	(NB)	(W)	(W)	
Ag/AgCl	0.02 M TPnACl	0.1 M TPnATPB	0.1 M LiCl	0.1 M LiCl	Ag/AgCl
(RE1)	0.1 M $MgSO_4$	10 mM Fc			(RE2)

Cell B

The counter electrode for the NB phase was a Pt coil electrode directly immersed in the phase, whereas that for the W phase was also a Pt coil electrode, which was immersed in a 0.1 M LiCl solution connected with the W phase through a glass sinter. Fc^+ was generated in the NB phase by electrolysis with a Pt disk electrode (surface area, 0.071 cm^2), which was located as close as 1 mm from the NB/W interface. The electrode potential of the Pt disk electrode was controlled in a three-electrode configuration with RE1 and the above Pt coil counter electrode immersed in NB. After 10-min electrolysis at +0.70 V, the transfer of Fc^+ across the NB/W interface was voltammetrically observed using cell B in a four-electrode configuration.

It has been claimed that the organic supporting-electrolyte anion used in the above measurements (i.e., TPB^-) had a catalytic influence on the reduction of Fc^+ in 1,2-DCE.[8,37] In our preliminary study, however, no distinct influence was observed in a voltammetric oxidation of Fc at Pt electrode in the NB solution containing 0.1 M TPnATPB. A supplementary experiment where TPnATPB was changed with the tetrakis(4-chlorophenyl)borate salt (known as a more stable electrolyte) was also performed for a typical case as shown later in Figure 1A. However, no marked difference was observed, and the validity of the use of TPnATPB as the organic supporting electrolyte in NB was shown.

For all the electrochemical measurements, test solutions were purged with N_2 gas, and electrolytic cells were thermostated at 25.0 ± 0.1 °C.

Digital Simulation of Cyclic Voltammograms. Calculations of cyclic voltammograms were performed by a normal explicit finite difference (EFD) digital simulation technique[38,39] with an exponentially expanding space grid method[39,40] (see Appendix). Simulation programs were written in Microsoft Visual Basic and used for manual curve-fitting analyses. Generally, in digital simulation for a system including chemical reaction(s), the calculation interval of potential, ΔE, should be made small enough that the calculated voltammogram is not dependent on ΔE. In this study, ΔE was set at 5−100 nV. Validity of a

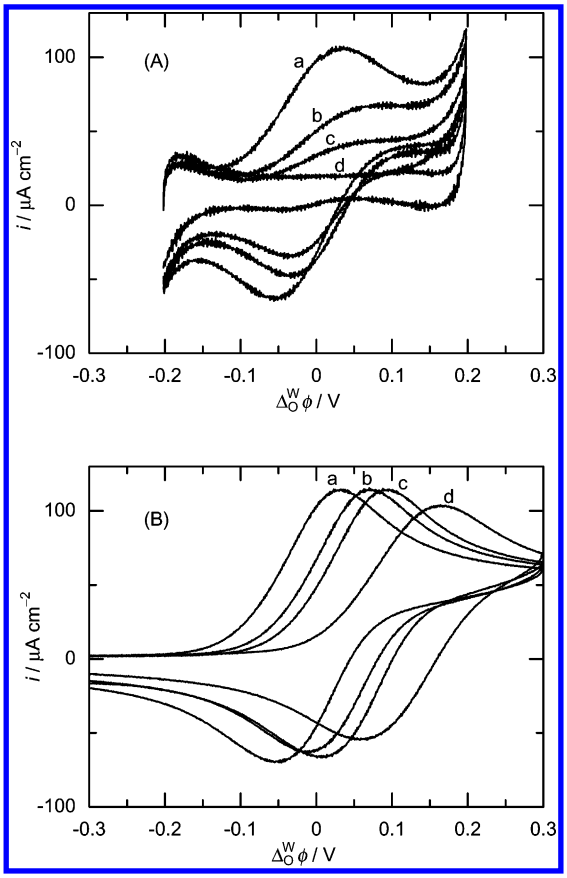

Figure 1. Cyclic voltammograms observed with (A) the O/W interface and (B) the corresponding ECSOW system in the presence of (a) 100, (b) 20, (c) 10, and (d) 1 mM Fc in NB and 0.5 mM $Fe(CN)_6^{3-}$ + 0.1 mM $Fe(CN)_6^{4-}$ in W. Sweep rate: 0.1 V s^{-1}.

program for the reversible ET mechanism was checked by referring to the previous numerical analysis.[41]

In the calculation of cyclic voltammograms, the initial concentrations of redox species were regarded as their "added" concentrations. However, these conditions are not necessarily met for practical voltammetric measurements. For the IT mechanism (eqs 2a−2c), the transfer of the electrically neutral redox species (i.e., Fc) into W can proceed spontaneously, or, even without electrochemical control, until an equilibrium is attained. Nevertheless, the cyclic voltammograms calculated by using the equilibrium concentrations for the initial conditions were practically the same as those calculated by using the added concentrations. Also in experiments, the cyclic voltammograms for the Fc−$Fe(CN)_6^{3-}$ system were not affected by the standing time before starting a voltage sweep.

Distribution Experiment. The NB−W partition coefficient of Fc was determined by a solvent extraction experiment. Fc was initially added to 20 mL of NB so that the concentration became 0.05−0.5 M and then distributed to 70 mL of W. After standing overnight at 25 ± 0.1 °C, Fc in the W phase was back-extracted into 20 mL of *n*-hexane. Almost the whole solvent was evaporated using a rotary vacuum evaporator; to the resultant condensed Fc solution was then added 2 mL of NB. Finally, the concentration of Fc in the NB solution was determined spectrophotometrically (molar absorption coefficient: ϵ = 342 at 450 nm).

Spectrophotometric Measurements. A spontaneous redox reaction between Fc (NB) and $Fe(CN)_6^{3-}$ (W) under no electrochemical control was monitored by means of a photodiode array spectrophotometer (Shimadzu, MultiSpec-1500). The experimental setup was similar to that described previously.[42] An interface between a 0.8 mL NB solution of 100 mM Fc and 1.4 mL of pure water was formed in a 1 cm quartz cell, and both phases were stirred. After an hour, an aliquot of a condensed hexacyanoferrate(III)/(II) aqueous solution was injected to the W phase so that the concentrations became $[K_3Fe(CN)_6]_W$ = 5$[K_4Fe(CN)_6]_W$ = 10 mM, and then absorption spectra of the W phase were recorded at a time interval of 15 s.

Results

Kinetic Behaviors of the Cyclic Voltammograms. Figure 1 shows the cyclic voltammograms for (A) the O/W interface and (B) the ECSOW system in the presence of various concentrations (1−100 mM) of Fc in NB and 0.5 mM $Fe(CN)_6^{3-}$ + 0.1 mM $Fe(CN)_6^{4-}$ in W. At the highest Fc concentration (i.e., $[Fc]_O$ = 100 mM), the voltammetric waves observed with both the systems were almost identical in appearance. This clearly shows that these two systems are thermodynamically equivalent. Under such conditions, one cannot discuss the reaction mechanism.

As shown previously,[33] the voltammetric behavior observed for the ECSOW system can be well elucidated by assuming reversible redox reactions at the Pt electrode surfaces in the O and W phases:

$$Fc(O) \rightleftharpoons Fc^+(O) + e^- \quad (3a)$$

$$Fe(CN)_6^{3-}(W) + e^- \rightleftharpoons Fe(CN)_6^{4-}(W) \quad (3b)$$

The voltammograms shown in Figure 1B could be completely reproduced by digital simulation[33] in which the equilibrium electromotive force of the ECSOW system is given by the Nernst equation:

$$E = E_{ET}^{\circ\prime} + \frac{RT}{nF}\ln\left(\frac{[R1]_W[O2]_O}{[O1]_W[R2]_O}\right) \quad (4)$$

where O1 = $Fe(CN)_6^{3-}$, R1 = $Fe(CN)_6^{4-}$, R2 = Fc, and O2 = Fc^+; the brackets [ ]$_W$ and [ ]$_O$ denote the equilibrium concentrations of the redox species in the W and O phases, respectively; *n* is the number of electrons involved in the interfacial redox reaction (here, *n* = 1); *R*, *T*, and *F* have their usual meanings; and $E_{ET}^{\circ\prime}$ is the formal potential determined by

$$\begin{aligned} E_{ET}^{\circ\prime} &= (E_{O2/R2}^{\circ\prime} - E_{O1/R1}^{\circ\prime}) + \Delta E_{ref} \\ &= \Delta_O^W\phi_{ET}^{\circ\prime} + \Delta E_{ref} \\ &= \Delta_O^W\phi_{ET}^{\circ} + \frac{RT}{nF}\ln\left(\frac{\gamma_{R1}^W\gamma_{O2}^O}{\gamma_{O1}^W\gamma_{R2}^O}\right) + \Delta E_{ref} \end{aligned} \quad (5)$$

Here, $E_{O2/R2}^{\circ\prime}$ and $E_{O1/R1}^{\circ\prime}$ are the formal potentials of the redox couples in the respective phases, which are expressed on the same potential scale; $\Delta_O^W\phi_{ET}^{\circ\prime}$ and $\Delta_O^W\phi_{ET}^{\circ}$ are the formal and standard redox potentials for the ET system, γ_i^α (α = W or O) is the activity coefficient of redox species *i* in the α phase, and ΔE_{ref} is a constant which is determined only by the reference electrodes used. In this study, all interfacial potentials refer to the midpoint potential (=0.546 V in cell A) for the reversible transfer of tetramethylammonium (TMA^+) ion from W to NB, whose standard ion-transfer potential ($\Delta_O^W\phi_{TMA}^{\circ}$) is known to be +0.035 V.[43] Then, ΔE_{ref} for cell A was evaluated to be 0.502

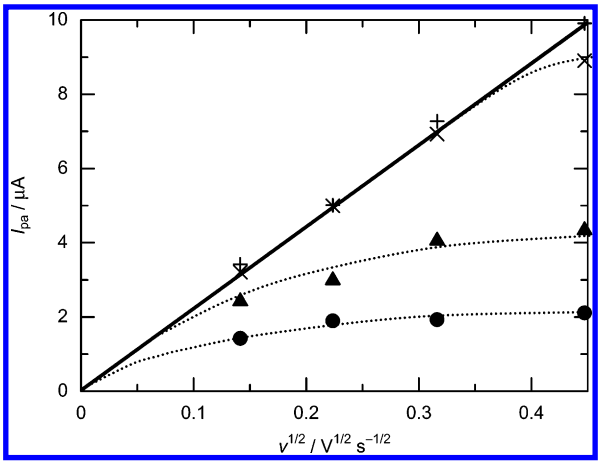

Figure 2. Sweep rate dependence of the anodic peak current for the voltammograms observed with the O/W interface in the presence of (+) 200, (×) 100, (▲) 20, and (●) 10 mM Fc in NB and 0.5 mM $Na_3Fe(CN)_6$ + 0.1 mM $Na_4Fe(CN)_6$ in W.

V in a manner similar to that described previously.[35] By fitting the simulation curves into experimental voltammograms in Figure 1B, the standard potential of the heterogeneous ET could be determined as $E_{ET}^{\circ\prime} = 0.625$ V in cell A,[33] i.e., $\Delta_O^W\phi_{ET}^{\circ\prime} = 0.123$ V; the diffusion coefficients of Fc in the NB phase and of $Fe(CN)_6^{3-}$ and $Fe(CN)_6^{4-}$ in the W phase were determined beforehand as 0.56×10^{-5}, 0.90×10^{-5}, and 0.57×10^{-5} cm s^{-1}, respectively, by conventional cyclic voltammetry (for Fc) or normal pulse voltammetry (for others) using a platinum disk electrode.

In contrast to the ECSOW system usually showing the reversible ET, the O/W interface gave kinetically controlled voltammograms under certain conditions; when the Fc concentration was decreased, the anodic peak current (I_{pa}) was significantly depressed and showed plateau, as seen in Figure 1A. This result is essentially the same as reported previously by Samec et al.[3] Figure 2 shows the dependence of I_{pa} on the square root of the voltage sweep rate (v). At higher Fc concentrations (i.e., $[Fc]_O = 200$ and 100 mM), the I_{pa} vs $v^{1/2}$ plot shows an almost straight line crossing the origin expected for the diffusion-controlled current; however, at lower Fc concentrations (20 and 10 mM), the plot deviated too much from the straight line even at lower v's.

Digital Simulation Analysis Based on the ET Mechanism. First, we assumed a simple heterogeneous ET mechanism to simulate cyclic voltammograms using the digital simulation technique.[38,39] In this case, the second-order rate constants of the forward (k_f) and backward (k_b) reactions of eq 1 are given by the Butler−Volmer equations:

$$k_f = k^\circ \exp\left[\frac{(1-\alpha)nF}{RT}(\Delta_O^W\phi - \Delta_O^W\phi_{ET}^{\circ\prime})\right] \quad (6a)$$

$$k_b = k^\circ \exp\left[-\frac{\alpha nF}{RT}(\Delta_O^W\phi - \Delta_O^W\phi_{ET}^{\circ\prime})\right] \quad (6b)$$

where k° is the standard rate constant at $\Delta_O^W\phi = \Delta_O^W\phi_{ET}^{\circ\prime}$, and α is the transfer coefficient. Using k° and α as adjusting parameters and the beforehand-determined standard potential and diffusion coefficients, we performed a manual curve-fitting analysis for the voltammograms shown in Figure 1A. Only when α was assumed to be close to unity (with $k^\circ = 0.12$ M^{-1} cm s^{-1} and $\Delta_O^W\phi_{ET}^{\circ\prime} = 0.123$ V) was a satisfactory result achieved, as shown in Figure 3A. The α value of unity is rather different

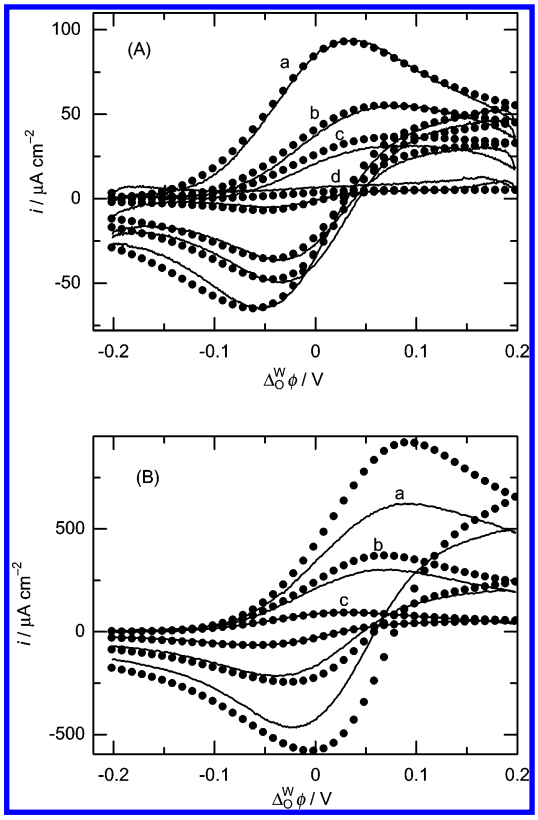

Figure 3. Baseline corrected cyclic voltammograms observed with the O/W interface by changing the concentration of (A) Fc in NB or (B) $Na_3Fe(CN)_6$ in W. (A) $[Fc]_O$ = (a) 100, (b) 20, (c) 10, and (d) 1 mM; $[Na_3Fe(CN)_6]_W = 5 \times [Na_4Fe(CN)_6]_W = 0.5$ mM. (B) $[Fc]_O$ = 100 mM; $[Na_3Fe(CN)_6]_W = 5 \times [Na_4Fe(CN)_6]_W$ = (a) 5, (b) 2, and (c) 0.5 mM. Sweep rate: 0.1 V s^{-1}. The solid circles in either (A) or (B) show the simulation data obtained by assuming the Butler−Volmer formalism. The adjusting parameters used are $k^\circ = 0.12$ M^{-1} cm s^{-1} and $\alpha = 1.0$; the others are as described in the text.

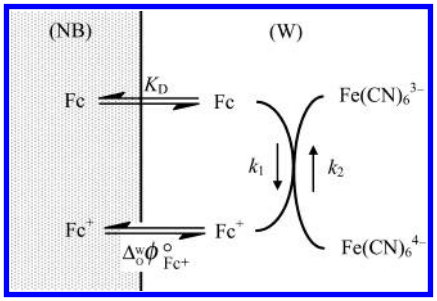

Figure 4. Reaction scheme of the IT mechanism for the Fc (NB)−$Fe(CN)_6^{3-}$ (W) system. For details, see the text.

from the value of 0.56 that is expected from the Marcus theory (see Discussion).[22] Furthermore, when the concentration of $Fe(CN)_6^{3-}$ in the W phase was changed in turn from 0.5 to 5 mM at a constant $[Fc]_O$ (=100 mM), the observed voltammograms could not be simulated using the same parameter set as in Figure 3A (see Figure 3B which represents large deviations between the simulation and experimental curves). This is the case for the voltammograms recorded under the concentration conditions reverse to those in Figure 3A,B, i.e., $[Fc] < [Fe(CN)_6^{3-}]$ (data not shown). Thus, the interfacial ET mechanism (eq 1) could not give a good explanation for the present system.

Digital Simulation Analysis Based on the IT Mechanism. We then employed the IT mechanism (eqs 2a−2c) to perform a digital simulation analysis. The IT mechanism is represented schematically in Figure 4. In the present analysis, the distribution

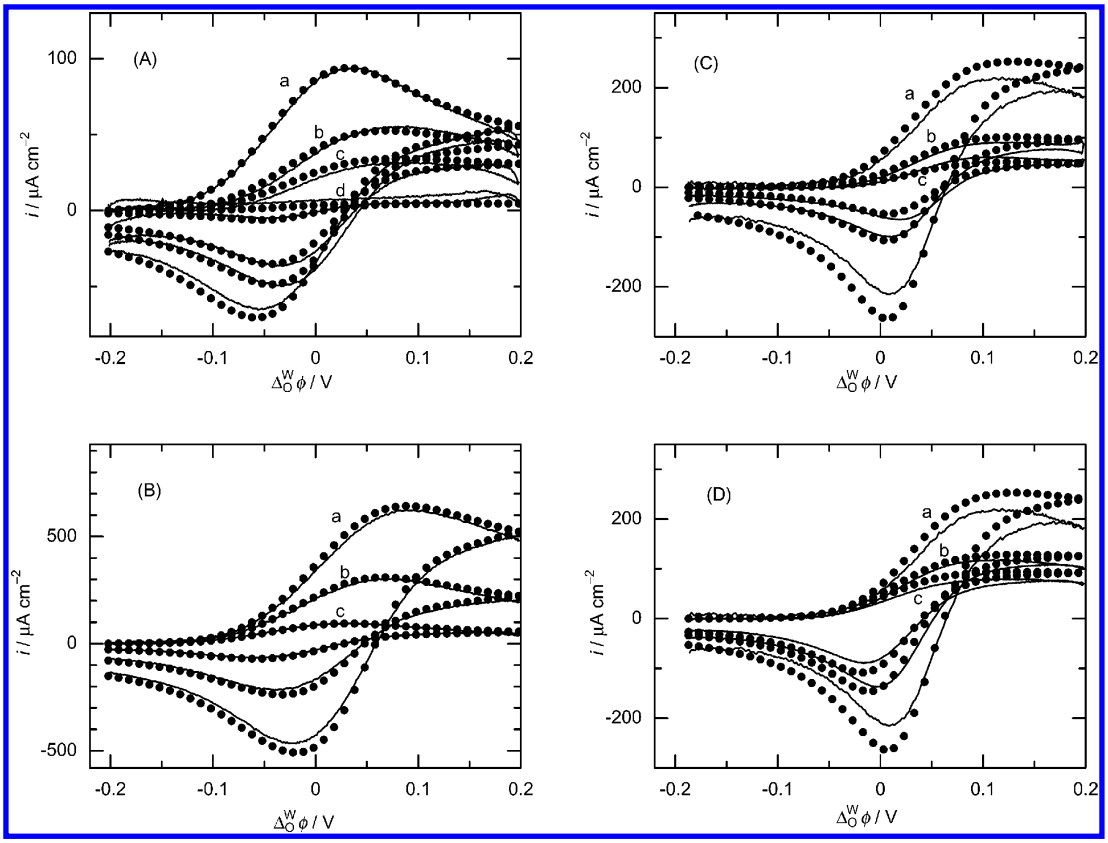

Figure 5. Baseline corrected cyclic voltammograms observed with the O/W interface: (A, C) by changing the Fc concentration in NB; (B, D) by changing the $Na_3Fe(CN)_6$ concentration in W. The concentration conditions in (A) and (B) are the same as those in Figure 3A,B, respectively. (C) $[Fc]_O$ = (a) 5, (b) 2, and (c) 1 mM; $[Na_3Fe(CN)_6]_W = 5 \times [Na_4Fe(CN)_6]_W = 100$ mM. (D) $[Fc]_O = 5$ mM; $[Na_3Fe(CN)_6]_W = 5 \times [Na_4Fe(CN)_6]_W$ = (a) 100, (b) 20, and (c) 10 mM. Sweep rate: 0.1 V s^{-1}. The solid circles show the regression data obtained by assuming the IT mechanism shown in Figure 4.

of Fc at the O/W interface was assumed to be always in equilibrium, i.e.,

$$\frac{[Fc]_O}{[Fc]_W} = K_D(\text{constant}) \tag{7}$$

The value of K_D was independently determined to be 6×10^3 by the solvent extraction experiment described above. This value is somewhat larger than a literature value[31] of 1.2×10^3, but in good agreement with another value[44] of 7×10^3.

Because the interfacial IT reaction is generally very fast, the IT of Fc^+ (=O2) across the O/W interface was assumed to obey the Nernst equation:

$$\Delta_O^W\phi = \Delta_O^W\phi^\circ_{Fc^+} + \frac{RT}{F}\ln\left(\frac{\gamma^O_{Fc^+}}{\gamma^W_{Fc^+}}\right) + \frac{RT}{F}\ln\left(\frac{[Fc^+]_O}{[Fc^+]_W}\right)$$

$$= \Delta_O^W\phi^{\circ\prime}_{Fc^+} + \frac{RT}{F}\ln\left(\frac{[Fc^+]_O}{[Fc^+]_W}\right) \tag{8}$$

The formal ion-transfer potential of Fc^+ ($\Delta_O^W\phi^{\circ\prime}_{Fc^+}$) was determined to be −0.096 V, as described above. This value is in reasonable agreement with a literature value[12] of −0.075 V. In the digital simulation, eq 8 was employed for relating the "interfacial" concentrations of Fc^+ in the two phases (see Appendix; eq A18); however it should be valid also for the "equilibrium" concentrations.

The kinetically controlled process in the IT mechanism is the homogeneous ET between Fc and $Fe(CN)_6^{3-}$ in the W phase. The reaction rate (v_{hom}) is expressed as

$$v_{hom} = -\frac{d[R2]_W}{dt} = \frac{d[O2]_W}{dt} = -\frac{d[O1]_W}{dt} = \frac{d[R1]_W}{dt}$$

$$= k_1[R2]_W[O1]_W - k_2[O2]_W[R1]_W \tag{9}$$

where t is the time, and k_1 and k_2 are the forward and backward second-order rate constants, respectively. In equilibrium (i.e., $v_{hom} = 0$), we obtain

$$\frac{[R1]_W[O2]_W}{[O1]_W[R2]_W} = \frac{k_1}{k_2} = K_{hom} \tag{10}$$

When the overall ET reaction across the O/W interface is in equilibrium, eq 4 should be valid regardless of the reaction mechanism adopted. Therefore, we can rewrite eq 4 for the present case, by replacing E and $E^{\circ\prime}_{ET}$ with $\Delta_O^W\phi$ and $\Delta_O^W\phi^{\circ\prime}_{ET}$, respectively:

$$\Delta_O^W\phi = \Delta_O^W\phi^{\circ\prime}_{ET} + \frac{RT}{F}\ln\left(\frac{[R1]_W[O2]_O}{[O1]_W[R2]_O}\right) \tag{11}$$

We assume for simplicity that $\gamma^W_{O1}/\gamma^W_{R1} = \gamma^O_{O2}/\gamma^O_{R2} = 1$ and $\gamma^O_{O2}/\gamma^W_{O2} = 1$, and then obtain from eqs 7, 8, 10, and 11 the following relation:

$$K_D \exp\left[\frac{F}{RT}(\Delta_O^W\phi^{\circ\prime}_{Fc^+} - \Delta_O^W\phi^{\circ\prime}_{ET})\right] = K_{hom} = \frac{k_1}{k_2} \tag{12}$$

By substituting to eq 12 the known-values of $\Delta_O^W\phi^{\circ\prime}_{Fc^+}$ and

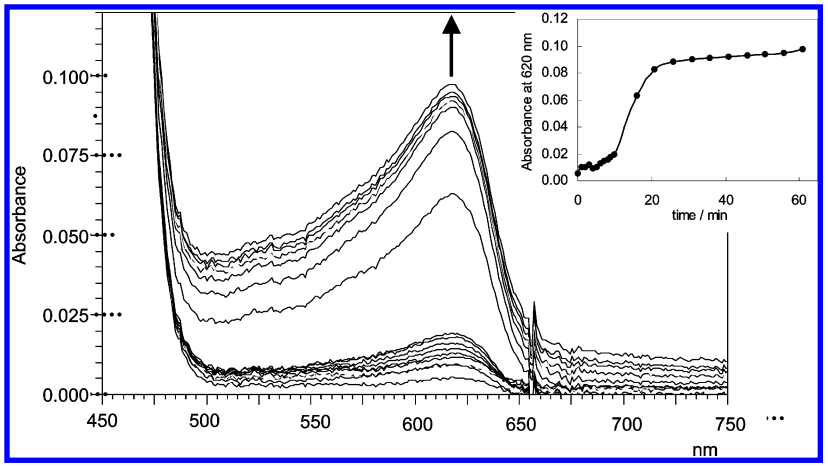

Figure 6. Absorption spectrum change of the W phase without electrochemical control. $[Fc]_O = 100$ mM; $[K_3Fe(CN)_6]_W = 5 \times [K_4Fe(CN)_6]_W = 10$ mM. The absorption spectra were recorded at a time interval of 15 s. The inset shows the time dependence of the absorbance at 620 nm.

$\Delta_O^W\phi_{ET}^{o\prime}$, K_{hom} was estimated to be 1.19. This value is in good agreement with that calculated from the redox potential difference between Fc^+/Fc in water (0.40 V vs NHE[12]) and $Fe(CN)_6^{3-}/Fe(CN)_6^{4-}$ (0.41 V vs NHE; in this study). As seen in eq 12, k_1 and k_2 are related with each other, therefore the unknown parameter is only k_1 (or, alternatively, k_2). The diffusion coefficients of Fc and Fc^+ in W required for the digital simulation were assumed to be identical and estimated to be 1.2×10^{-5} cm^2 s^{-1} from the diffusion coefficient of Fc in NB ($D^{NB} = 0.56 \times 10^{-5}$ cm^2 s^{-1} [33]) on the assumption that $D^W/D^{NB} = 2$ (i.e., the reciprocal of the viscosity ratio of water and NB).

In this manner, we carried out digital simulation using a sole fitting parameter (i.e., k_1). When k_1 was set to be 2.0×10^7 M^{-1} s^{-1}, the curve fitting was successful for the voltammograms observed under any concentration conditions (Figure 5A−D). It should be stressed that the same parameter set was employed for the calculation of all sets of voltammograms.

Spectrophotometric Measurement. If the IT mechanism is valid, the reaction steps other than the IT of Fc^+ should occur spontaneously without electrochemical control. In practice, an absorption spectrum change of the W phase could be observed as shown in Figure 6. The absorption peak around 620 nm increased with time until it reached an equilibrium value (see the inset of Figure 6). This undoubtedly showed the formation of Fc^+ in the W phase, because a flow-column electrolysis of Fc in water-acetone revealed that Fc^+ had an absorption maximum at 620 nm. This result would also support the IT mechanism.

Discussion

The above results clearly showed that in the $Fc-Fe(CN)_6^{3-}$ system, ET should occur not at the O/W interface but in the W phase. To verify this, we further calculated the concentration profiles of Fc^+ and Fc, on the basis of the above-mentioned digital simulation of cyclic voltammograms. Figure 7 shows a snapshot of the concentration profiles of Fc^+ and Fc at $\Delta_O^W\phi = 0.14$ V, which was obtained for a typical voltammetric sweep at 0.1 V s^{-1}. As can be seen in the figure, the concentration of either Fc^+ or Fc in the W phase shows a maximum at ca. 80 μm, as a consequence of the competitive ET and diffusion. It should be noted that the reaction layer in the W phase grows to ca. 200 μm in the course of the voltammetric sweep of a few seconds. In contrast, the reaction field for the heterogeneous

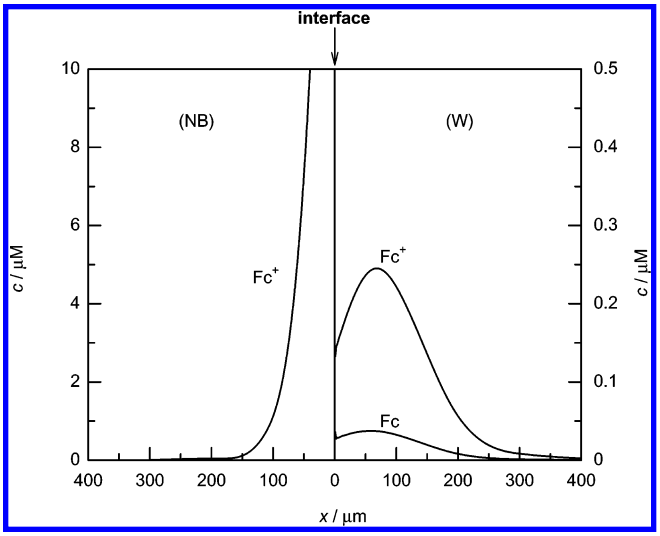

Figure 7. Snapshot of concentration profiles of Fc and Fc^+, obtained by the digital simulation based on the IT mechanism, at $\Delta_O^W\phi = 0.14$ V (i.e., 3.4 s after a voltammetric sweep at 0.1 V s^{-1}). Initial conditions: $[Fc]_O = 1.0$ mM, $[Fe(CN)_6^{3-}]_W = 5 \times [Fe(CN)_6^{4-}]_W = 0.5$ mM. Though not evident in the figure, the Fc concentration in W at around 0 μm suddenly drops from ~0.16 to ~0.03 μM. The concentration profile of Fc in NB is omitted.

ET should be restricted to an interfacial layer as thin as several ångstroms. Therefore, the volume of reaction field for the homogeneous ET would be ~10^6 times larger than that for the heterogeneous ET. Such a large difference in the volume of reaction field leads to the most crucial advantage of the IT mechanism, which would overcome its disadvantage, i.e., the small partition of Fc into the W phase (cf. $K_D = 6 \times 10^3$).

Thus the volume of reaction field is a key factor for determining the reaction pathway or mechanism, but it would be worthwhile to consider theoretically the rate constants of the heterogeneous as well as homogeneous ETs. Recently, we have proposed a theoretical equation for the diffusion-controlled rate constant of heterogeneous ET at the O/W interface by extension of the Smoluchowski−Debye theory[45,46] for a bimolecular reaction in homogeneous solution. In the proposed theory,[34] the diffusion-controlled (i.e., realizable maximum) rate constant, $k_{D,het}$, is given by

$$k_{D,het} = 8\pi r_A r_{AB} \xi D_B^W L \qquad (13)$$

in the case where the reaction rate is limited by the diffusion of

the redox species (B) in W. In eq 13, r_A is the radius of the redox species (A) in O, D_B^W is the diffusion coefficient of the redox species (B) in W, r_{AB} (=$r_A + r_B$) is the sum of the radii of A and B, L is Avogadro's number, and ξ is defined as

$$\xi = \frac{1 - \cos\theta}{2} \tag{14}$$

with

$$\theta = \cos^{-1}\left(\frac{r_A}{r_{AB}}\right) \tag{15}$$

Reversely, if the reaction rate is limited by the diffusion of A in O, $k_{D,het}$ is likewise given by

$$k_{D,het} = 8\pi r_B r_{AB} \xi D_A^O L \tag{16}$$

where D_A^O is the diffusion coefficient of A in O and ζ is defined by

$$\zeta = \frac{1 - \cos\omega}{2} \tag{17}$$

with

$$\omega = \cos^{-1}\left(\frac{r_B}{r_{AB}}\right) \tag{18}$$

Using the following parameters, $r_A = 3.8 \times 10^{-8}$ cm,[47] $r_B = 4.4 \times 10^{-8}$ cm,[48] $D_A^O = 0.56 \times 10^{-5}$ cm^2 s^{-1},[33] and $D_B^W = 0.90 \times 10^{-5}$ cm^2 s^{-1},[33] the $k_{D,het}$ value can be estimated for the Fc (NB)−Fe(CN)$_6^{3-}$ (W) system (note here that A = Fc and B = Fe(CN)$_6^{3-}$). In the use of eq 16 with eqs 17 and 18, $k_{D,het}$ is calculated to be 71 M^{-1} cm s^{-1}, which is smaller than the value of 114 M^{-1} cm s^{-1} calculated using eq 13 with eqs 14 and 15. Accordingly, the $k_{D,het}$ for the present system is considered as 71 M^{-1} cm s^{-1}.

Previously, Marcus[21−25] derived an Arrhenius-type general kinetic equation for heterogeneous ET at a sharp O/W interface:

$$k = Z\exp\left(\frac{-\Delta G^{\ddagger}}{RT}\right) = 2\pi(r_A + r_B)\kappa\nu(\Delta R)^3 \exp\left(\frac{-\Delta G^{\ddagger}}{RT}\right) \tag{19}$$

where k is the second-order rate constant, κ is the Landau−Zener nonadiabacity factor, ν is the relevant frequency for molecular motion, ΔR appears in an exponent for the dependence of the ET rate on separation distance R ($\propto \exp(-R/\Delta R)$), and $\Delta G^{\ddagger}$ is the standard Gibbs energy of activation of the reaction. The preexponential frequency factor $Z = 2\pi(r_A + r_B)\kappa\nu(\Delta R)^3$ is the "maximum" value of k at $\Delta G^{\ddagger} = 0$ (not necessarily realizable), and it is interesting to compare the Z factor with the value of $k_{D,het}$. Using $\kappa\nu = 10^{12}$ s^{-1} and $\Delta R = 1 \times 10^{-8}$ cm, which were adopted by Marcus,[23] the Z factor is calculated to be 310 M^{-1} cm s^{-1} for the Fc−Fe(CN)$_6^{3-}$ system. This value is about 4 times larger than the $k_{D,het}$ value estimated above (i.e., 71 M^{-1} cm s^{-1}).

In the following, we calculate the standard rate constant by using the Marcus theory. In the calculation, $\Delta G^{\ddagger}$ has been evaluated by[22]

$$\Delta G^{\ddagger} = w^r + \frac{\lambda}{4}\left(1 + \frac{\Delta G^{\circ} + w^p - w^r}{\lambda}\right)^2 \tag{20}$$

where w^r and w^p are the work terms for bringing the reactants from d (the distance between two reactants) = ∞ and for removing the products to $d = \infty$, respectively, λ is the reorganization energy estimated from the sum of the contributions of outer (λ_o) and inner (λ_i) spheres, and ΔG° is the standard Gibbs energy expressed as $-F(\Delta_O^W\phi - \Delta_O^W\phi^{\circ})$. Substituting into eq 20 the values $w^r = 3.4$ kJ mol^{-1},[49] $w^p = -6.8$ kJ mol^{-1},[49] $\lambda_o = 78.8$ kJ mol^{-1},[50] λ_i(Fc) = 0.6 kJ mol^{-1},[51] λ_i(Fe(CN)$_6^{3-/4-}$) = 10.6 kJ mol^{-1},[52] and $\Delta G^{\circ} = 0$ yields $\Delta G^{\ddagger} = 18.5$ kJ mol^{-1} at $\Delta_O^W\phi = \Delta_O^W\phi^{\circ} \approx \Delta_O^W\phi_{ET}^{\circ\prime}$. Using the above estimated Z factor (=310 M^{-1} cm s^{-1}), the standard rate constant, k° (i.e., k at $\Delta_O^W\phi = \Delta_O^W\phi_{ET}^{\circ\prime}$) is estimated to be 0.064 M^{-1} cm s^{-1}. This k° value is comparable with the experimental value (0.12 M^{-1} cm s^{-1}), which was tentatively obtained by assuming the ET mechanism. However, we should direct our attention not only to the k° value but also to the α value, which will be evaluated on the basis of the Marcus theory as follows: Substituting $-F(\Delta_O^W\phi - \Delta_O^W\phi^{\circ})$ for ΔG° in eq 20 yields

$$\Delta G^{\ddagger} = \Delta G^{\circ\ddagger} - \frac{1}{2}F(\Delta_O^W\phi - \Delta_O^W\phi^{\circ}) + \frac{1}{4\lambda}\{F^2(\Delta_O^W\phi - \Delta_O^W\phi^{\circ})^2 - 2F(\Delta_O^W\phi - \Delta_O^W\phi^{\circ})(w^p - w^r)\} \tag{21}$$

where $\Delta G^{\circ\ddagger}$ stands for $\Delta G^{\ddagger}$ at $\Delta_O^W\phi = \Delta_O^W\phi^{\circ}$. When $F|\Delta_O^W\phi - \Delta_O^W\phi^{\circ}|/2\lambda \ll 1$, eq 21 is reduced to

$$\Delta G^{\ddagger} = \Delta G^{\circ\ddagger} - \frac{1}{2}\left(1 + \frac{w^p - w^r}{\lambda}\right)F(\Delta_O^W\phi - \Delta_O^W\phi^{\circ}) \tag{22}$$

Comparing this equation with the following relation in the classical Butler−Volmer formalism (note that $\Delta_O^W\phi^{\circ} \approx \Delta_O^W\phi_{ET}^{\circ\prime}$),

$$\Delta G^{\ddagger} = \Delta G^{\circ\ddagger} - (1 - \alpha)F(\Delta_O^W\phi - \Delta_O^W\phi_{ET}^{\circ\prime}) \tag{23}$$

and using the above w^r, w^p, and λ, we can calculate α to be 0.56. As described above, however, the α value obtained by assuming the ET mechanism is unity, being rather different from the theoretically expected value. This would also imply the validity of the ET mechanism (eq 1) for the present system, although the effect of the electric double layer[15] should be considered for a more rigorous discussion.

On the other hand, the homogeneous ET rate constant obtained by the fitting analysis of cyclic voltammograms based on IT mechanism is $k_1 = 2 \times 10^7$ M^{-1} s^{-1}. Although there is no literature about the rate constant for the Fc−Fe(CN)$_6^{3-}$ reaction in W, some rate constants ranging from 10^5 to $>10^8$ M^{-1} s^{-1} were reported for other bimolecular redox reactions in aqueous media in which hexacyanoferrates participate.[53] Also, the k_1 value is 3 orders lower than the diffusion-controlled rate constant (1.3×10^{10} M^{-1} s^{-1}) calculated by the Smoluchowski−Debye theory.[45,46] Thus, the k_1 value seems reasonable enough to conclude that the Fc (NB)−Fe(CN)$_6^{3-}$ (W) system can be well elucidated in terms of the IT mechanism.

As is evident from the above discussion, however, the reaction mechanism would be affected by hydrophobicity of the redox species in the O phase. The larger the K_D value, the more difficult to occur the homogeneous ET. If we use an extremely hydrophobic redox species in the O phase, the IT mechanism would not occur, and thus a heterogeneous ET would be realized. Further voltammetric studies are now in progress with some Fc derivatives substituted by methyl groups and other metal complexes.

Appendix

Digital Simulation of Cyclic Voltammograms. The EFD method[38,39] was used to calculate cyclic voltammograms for the ET and IT mechanisms. In the calculation, we constructed a discrete model featuring two sequences of volume elements extending away from the O/W interface to the respective bulk phases. To shorten the calculation time, the exponentially expanding grid method[39,40] was used, in which the discretized distance (Δx) for a volume element is given by

$$\Delta x(j) = \Delta x \exp[\beta(j-1)] \tag{A1}$$

where j (=1, 2, 3, ...) is the finite difference parameter for distance, and β is an arbitrary parameter ($\beta = 0.5$ for the IT mechanism, but $\beta = 0$ for the ET mechanism).

If there is no homogeneous ET reaction, the diffusion problem for a redox species, i, in phase X (=O or W) can be written in the finite difference form of Fick's second law: for $j \geq 2$,

$$f_i^X(j,k+1) = f_i^X(j,k) + \mathbf{D}_i^X(j)'[f_i^X(j+1,k) - f_i^X(j,k)] - \mathbf{D}_i^X(j)''[f_i^X(j,k) - f_i^X(j-1,k)] \tag{A2}$$

and for $j = 1$,

$$f_i^X(1,k+1) = f_i^X(1,k) + \mathbf{D}_i^X(1)'[f_i^X(2,k) - f_i^X(1,k)] + J_i(0,k) \tag{A3}$$

In these equations, $f_i^X(j,k)$ is the "dimensionless" concentration of species i in the jth element of phase X at the time of $k\Delta t$ (with $k = 0, 1, 2, ...$; Δt being the discretized time), which is defined by the relative concentration of the species with respect to the total concentration (C_{total}) for all the redox species involved in the O/W system, and $\mathbf{D}_i^X(j)'$ and $\mathbf{D}_i^X(j)''$ are defined as follows using the diffusion coefficient of species i in phase X (D_i^X), the maximum value among the D_i^X values for all species (D_{max}), and the model diffusion coefficient ($\mathbf{D}_M$):[39]

$$\mathbf{D}_i^X(j)' = \mathbf{D}_M \frac{D_i^X}{D_{max}} \exp\left[2\beta\left(\frac{3}{4} - j\right)\right] \tag{A4}$$

$$\mathbf{D}i^X(j)'' = \mathbf{D}_M \frac{D_i^X}{D_{max}} \exp\left[2\beta\left(\frac{5}{4} - j\right)\right] \tag{A5}$$

$$\mathbf{D}_M \equiv \frac{D_i^X \Delta t}{(\Delta x)^2} = 0.45 \tag{A6}$$

Finally, the remaining term in eq A3, $J_i(0,k)$, is the dimensionless flux of species i across the interface written in the finite difference form of Fick's first law:

$$J_i(0,k) = -2\mathbf{D}_i^X(1)''[f_i^X(1,k) - f_i^X(0,k)] \tag{A7}$$

At the calculation, we first give the calculation interval of potential (ΔE), and then Δx is set by eq A6 with $\Delta t = \Delta E/\upsilon$ (υ, voltage sweep rate).

In the ET mechanism, it is assumed that the heterogeneous ET reaction:

$$\mathrm{O1(W)} + \mathrm{R2(O)} \rightleftharpoons \mathrm{R1(W)} + \mathrm{O2(O)} \tag{A8}$$

occurs only at the nearest array to the interface ($j = 0$), and the ET rate constants of the forward and backward reactions are given by the Butler−Volmer equations (eqs 6a and 6b). The dimensionless flux of a redox species (e.g., O1) is then given by

$$J_{O1} = -k_f' f_{O1}^W(0,k)\, f_{R2}^O(0,k) + k_b' f_{R1}^W(0,k)\, f_{O2}^O(0,k) \tag{A9}$$

where k_f' and k_b' are the dimensionless rate constants defined by multiplying k_f or k_b (eqs 6a and 6b) by $C_{total}\Delta t/\Delta x$. Considering the mass balance at the interface, we obtain

$$-J_{O1}(0,k) = -J_{R2}(0,k) = J_{R1}(0,k) = J_{O2}(0,k) = \frac{I(k)}{nFA} \cdot \frac{\Delta t}{C_{total}\Delta x} \tag{A10}$$

where $I(k)$ is the current at $k\Delta t$. The combination of eqs A7, A9, and A10 leads to the following quadratic equation for $J_{O1}(0,k)$:

$$AJ_{O1}(0,k)^2 - BJ_{O1}(0,k) + C = 0 \tag{A11}$$

with

$$A = -\frac{k_f'}{4\mathbf{D}_{O1}^W \mathbf{D}_{R2}^O} + \frac{k_b'}{4\mathbf{D}_{R1}^W \mathbf{D}_{O2}^O} \tag{A12}$$

$$B = \frac{k_f'}{2\mathbf{D}_{R2}^O} f_{O1}^W(1,k) + \frac{k_f'}{2\mathbf{D}_{O1}^W} f_{R2}^O(1,k) + \frac{k_b'}{2\mathbf{D}_{O2}^O} f_{R1}^W(1,k) + \frac{k_b'}{2\mathbf{D}_{R1}^W} f_{O2}^O(1,k) + 1 \tag{A13}$$

$$C = -k_f' f_{O1}^W(1,k)\, f_{R2}^O(1,k) + k_b' f_{R1}^W(1,k)\, f_{O2}^O(1,k) \tag{A14}$$

By solving eq A11, we can obtain $J_{O1}(0,k) = (B - \sqrt{B^2 - 4AC})/2A$ and thus $I(k)$ using eq A10.

In the IT mechanism where a homogeneous ET occurs in the W phase, the concentration change of species i due to the chemical reaction, $\Delta f_{i,CR}^W(j,k+1)$, was calculated by

$$\Delta f_{i,CR}^W(j,k+1) = k_1' f_{O1}^W(j,k)\, f_{R2}^W(j,k) - k_2' f_{R1}^W(j,k)\, f_{O2}^W(j,k) \quad (\text{for } j \geq 1) \tag{A15}$$

where k_1' and k_2' are the dimensionless rate constants which correspond to k_1 and k_2 (cf. eq 9). Independent of the effect of chemical reaction, the concentration change due to diffusion was treated, i.e.,

$$f_i^W(j,k+1) = f_{i,Diff}^W(j,k+1) \pm \Delta f_{i,CR}^W(j,k+1) \tag{A16}$$

where $f_{i,Diff}^W(j,k+1)$ was calculated using eq A2 or A3 for the case where there is no chemical reaction; the + sign corresponds to when i = O2 or R1, and the − sign to when i = O1 or R2.

The following relations were used for the distribution equilibria for Fc (=R2) and Fc^+ (= O2) at the interface (i.e., $j = 0$):

$$K_D = \frac{f_{R2}^O(0,k)}{f_{R2}^W(0,k)} \tag{A17}$$

and

$$\frac{f_{O2}^O(0,k)}{f_{O2}^W(0,k)} = \exp\left[\frac{F}{RT}(\Delta_O^W\phi(k) - \Delta_O^W\phi_{O2}^{\circ\prime})\right] = \theta \tag{A18}$$

where $\Delta_O^W\phi(k)$ is the Galvani potential difference of the interface at the time of $k\Delta t$. Considering the mass balance, we can obtain the following relations for the dimensionless fluxes of Fc and Fc^+ at the interface:

$$J_{R2}^W(0,k) = -J_{R2}^O(0,k) \tag{A19}$$

$$J_{O2}^O(0,k) = -J_{O2}^W(0,k) = \frac{I(k)}{FA}\cdot\frac{\Delta t}{C_{total}\Delta x} \tag{A20}$$

Finally, the combination of eqs A7, A17, and A19 for R2 leads to

$$J_{R2}^O(0,k) = \frac{-f_{R2}^O(1,k) + K_D f_{R2}^W(1,k)}{\frac{1}{2\mathbf{D}_{R2}^O(1)} + \frac{K_D}{2\mathbf{D}_{R2}^W(1)}} \tag{A21}$$

and the combination of eqs A7, A18, and A20 for O2 leads to

$$J_{O2}^O(0,k) = \frac{-f_{O2}^O(1,k) + \theta f_{O2}^W(1,k)}{\frac{1}{2\mathbf{D}_{O2}^O(1)} + \frac{\theta}{2\mathbf{D}_{O2}^W(1)}} \tag{A22}$$

This equation with eq A20 allows the calculation of I(k).

References and Notes

(1) Volkov, A. G.; Deamer, D. W.; Tanelian, D. L.; Markin V. S. *Liquid Interfaces in Chemistry and Biology*; Wiley: New York, 1998.

(2) *Liquid Interfaces in Chemical, Biological, and Pharmaceutical Applications*; Volkov, A. G., Ed.; Marcel Dekker: Boca Raton, FL, 2001.

(3) Samec, Z.; Mareček, V.; Weber, J. *J. Electroanal. Chem.* **1979**, *103*, 11.

(4) Kihara, S.; Suzuki, M.; Maeda, K.; Ogura, K.; Matsui, M.; Yoshida, Z. *J. Electroanal. Chem.* **1989**, *271*, 107.

(5) Geblewicz, G.; Schiffrin, D. J. *J. Electroanal. Chem.* **1988**, *244*, 27.

(6) Cunnane, V. J.; Schiffrin, D. J.; Beltran, C.; Geblewicz, G.; Solomon, T. *J. Electroanal. Chem.* **1988**, *247*, 203.

(7) Cheng, Y.; Schiffrin, D. J. *J. Electroanal. Chem.* **1991**, *314*, 153.

(8) Cunnane, V. J.; Geblewicz, G.; Schiffrin, D. J. *Electrochim. Acta* **1995**, *40*, 3005.

(9) Suzuki, M.; Umetani, S.; Matsui, M.; Kihara, S. *J. Electroanal. Chem.* **1997**, *420*, 119.

(10) Suzuki, M.; Matsui, M.; Kihara, S. *J. Electroanal. Chem.* **1997**, *438*, 147.

(11) Ohde, H.; Maeda, K.; Yoshida, Y.; Kihara, S. *Electrochim. Acta* **1998**, *44*, 23.

(12) Hanzlík, J.; Samec, Z.; Hovorka, J. *J. Electroanal. Chem.* **1987**, *216*, 303.

(13) Hanzlík, J.; Hovorka, J.; Samec, Z.; Toma, S. *Collect. Czech. Chem. Commun.* **1988**, *53*, 903.

(14) Quinn, B.; Kontturi, K. *J. Electroanal. Chem.* **2000**, *483*, 124.

(15) Samec, Z.; Mareček, V.; Weber, J.; Homolka, D. *J. Electroanal. Chem.* **1981**, *126*, 105.

(16) Chen, Q. Z.; Iwamoto, K.; Seno, M. *Electrochim. Acta* **1991**, *36*, 291.

(17) Quinn, B.; Lahtinen, R.; Murtomäki, L.; Kontturi, K. *Electrochim. Acta* **1998**, *44*, 47.

(18) Zhang, Z.; Yuan, Yi; Sun, P.; Su, B.; Guo, J.; Shao, Y. *J. Phys. Chem. B* **2002**, *106*, 6713.

(19) Chikama, K.; Nakatani, K.; Kitamura, N. *Bull. Chem. Soc. Jpn.* **1998**, *71*, 1065.

(20) Zhang, J.; Slevin, C. J.; Unwin, P. R. *Chem. Commun.* **1999**, 1501.

(21) Marcus, R. A. *J. Phys. Chem.* **1990**, *94*, 1050.

(22) Marcus, R. A. *J. Phys. Chem.* **1990**, *94*, 4152.

(23) Marcus, R. A. *J. Phys. Chem.* **1991**, *95*, 2010.

(24) Marcus, R. A. *J. Phys. Chem.* **1990**, *94*, 7742 (corrections).

(25) Marcus, R. A. *J. Phys. Chem.* **1995**, *99*, 5742 (corrections).

(26) Kharkatz, Y. I.; Kuznetsov, A. M. In *Liquid−Liquid Interfaces, Theory and Methods*; Volkov, A. G., Deamer, D. W., Eds.; CRC Press: Boca Raton, FL, 1996, Chapter 7.

(27) Volkov, A. G.; Deamer, D. W. *Prog. Colloid Polym. Sci.* **1997**, *103*, 221.

(28) Schmickler, W. *J. Electroanal. Chem.* **1997**, *428*, 123.

(29) Benjamin, I.; Kharkats, Y. I. *Electrochim. Acta* **1998**, *44*, 133.

(30) Cheng, Y.; Schiffrin, D. J. *J. Chem. Soc., Faraday Trans.* **1993**, *89*, 199.

(31) Wei, C.; Bard, A. J.; Mirkin, M. V. *J. Phys. Chem.* **1995**, *99*, 16033.

(32) Barker, A. L.; Unwin, P. R.; Amemiya, S.; Zhou, J.; Bard, A. J. *J. Phys. Chem. B* **1999**, *103*, 7260.

(33) Hotta, H.; Akagi, N.; Sugihara, T.; Ichikawa, S.; Osakai, T. *Electrochem. Commun.* **2002**, *4*, 472.

(34) Osakai, T.; Hotta, H. In *Interfacial Electrochemistry*; Watarai, H., Ed.; Kluwer Academic Publishers: Boston (in press).

(35) Osakai, T.; Himeno, S.; Saito, A. *J. Electroanal. Chem.* **1992**, *332*, 169.

(36) Aoyagi, S.; Matsudaira, M.; Suzuki, T.; Katano, H.; Sawada, S.; Hotta, H.; Ichikawa, S.; Sugihara, T.; Osakai, T. *Electrochemistry* **2002**, *70*, 329.

(37) Cunnane, V. J.; Murtomäki, L. In *Liquid−Liquid Interfaces, Theory and Methods*; Volkov, A. G., Deamer, D. W., Eds.; CRC Press: Boca Raton, FL, 1996; Chapter 18.

(38) Feldberg, S. W. In *Electroanalytical Chemistry*; Bard A. J., Ed.; Marcel Dekker: New York, 1969; Vol. 3, pp 199−296.

(39) Bard, A. J.; Faulkner, L. F. *Electrochemical Methods, Fundamentals and Applications*; Wiley: New York, 2001; p 785−806.

(40) Feldberg, S. W. *J. Electroanal. Chem.* **1981**, *127*, 1.

(41) Stewart, A. A.; Campbell, J. A.; Girault, H. H.; Eddowes, M. *Ber. Bunsen-Ges. Phys. Chem.* **1990**, *94*, 83.

(42) Osakai, T.; Akagi, N.; Hotta, H.; Ding, J.; Sawada, S. *J. Electroanal. Chem.* **2000**, *490*, 85.

(43) Koryta, J.; Vanýsek, P.; Březina, M. *J. Electroanal. Chem.* **1977**, *75*, 211.

(44) Nakatani, K.; Uchida, T.; Misawa, H.; Kitamura, N.; Masuhara, H. *J. Electroanal. Chem.* **1994**, *367*, 109.

(45) Smoluchowski, M. V. *Z. Phys. Chem.* **1917**, *92*, 129.

(46) Debye, P. *Trans. Electrochem. Soc.* **1942**, *82*, 265.

(47) Nielson, R. M.; McManis, G. E.; Golovin, M. N.; Weaver, M. J. *J. Phys. Chem.* **1988**, *92*, 3441.

(48) Marcus, Y. *Ion Properties*; Marcel Dekker: New York, 1997; Chapter 3.

(49) The values of w^r and w^p were calculated from eq 20 in ref 21 using the static and optical dielectric constants of NB (35.7 and 2.4, respectively) and those of water (78.3 and 1.8).

(50) The value of λ_o was calculated from eq 16 in ref 21.

(51) Gennett, T.; Milner, D. F.; Weaver, M. J. *J. Phys. Chem.* **1985**, *89*, 2787.

(52) Delahay, P. *Chem. Phys. Lett.* **1983**, *99*, 87.

(53) Pennington, D. E. In *Coordination Chemistry Volume 2*; Martell, A. E., Ed.; American Chemical Society: Washington, 1978; Chapter 3.